



Published in final edited form as:

Ann Surg Oncol. 2006 December ; 13(12): 1671–1681.

Image-Guided Oncologic Surgery Using Invisible Light: Completed Pre-Clinical Development for Sentinel Lymph Node Mapping

Eiichi Tanaka, MD, PhD¹, Hak Soo Choi, PhD¹, Hirofumi Fujii, MD, PhD¹, Mounqi G. Bawendi, PhD², and John V. Frangioni, MD, PhD^{1,3}

¹ Division of Hematology/Oncology, Department of Medicine, Beth Israel Deaconess Medical Center, Boston, MA 02215

³ Department of Radiology, Beth Israel Deaconess Medical Center, Boston, MA 02215

² Department of Chemistry, Massachusetts Institute of Technology, Cambridge, MA 02139

Abstract

Background—Invisible near-infrared (NIR) fluorescent light permits high sensitivity, real-time image-guidance during oncologic surgery without changing the look of the surgical field. In this study, we complete pre-clinical development of the technology for sentinel lymph node (SLN) mapping using a large animal model of spontaneous melanoma.

Methods—Sinclair swine with spontaneous melanoma metastatic to regional lymph nodes were used because of their similarity to human melanoma. Organic lymphatic tracers tested included FDA-approved indocyanine green adsorbed non-covalently to human serum albumin (HSA), and NIR fluorophore CW800 conjugated covalently to HSA (HSA800). The inorganic/organic hybrid tracer tested was type II NIR quantum dots with an anionic coating. Primary tumors received four peritumoral injections of each tracer, with a fluorophore dose of 100 pmol to 1 nmol per injection. SLN mapping and image-guided resection were performed in real-time.

Results—Each of the 3 lymphatic tracers was injected into $n = 4$ separate primary melanomas in a total of 6 animals. All 12 injections resulted in identification of the SLN(s) and their associated lymphatic channels within 1 minute in 100% of cases, despite highly pigmented skin and black fur. Hydrodynamic diameter had a profound impact on tracer behavior *in vivo*.

Conclusions—This study completes the pre-clinical development of NIR fluorescence-guided SLN mapping, and provides insight into imaging system optimization and tracer choice for future human clinical trials. The technology is likely to eliminate the need for radioactive and colored tracers, permits real-time image guidance throughout the procedure, and assists the pathologist in tissue analysis.

Keywords

Sentinel Lymph Node Mapping; Pre-Clinical Development; Near-Infrared Light; Near-Infrared Fluorescence; Melanoma; Sinclair Pigs

Corresponding Author: John V. Frangioni, MD, PhD Beth Israel Deaconess Medical Center 330 Brookline Avenue, Room SL-B05 Boston, MA 02215 Phone: 617-667-0692 Fax: 617-667-0981 E-mail: jfrangio@bidmc.harvard.edu.

Publisher's Disclaimer: This PDF receipt will only be used as the basis for generating PubMed Central (PMC) documents. PMC documents will be made available for review after conversion (approx. 2–3 weeks time). Any corrections that need to be made will be done at that time. No materials will be released to PMC without the approval of an author. Only the PMC documents will appear on PubMed Central -- this PDF Receipt will not appear on PubMed Central.

INTRODUCTION

The major “imaging system” presently used during oncologic surgery is the surgeon's eyes. The instruments required for computed tomography (CT), magnetic resonance imaging (MRI), single photon emission computed tomography (SPECT) and positron emission tomography (PET) are too large, expensive, and bulky for intraoperative use. Ultrasound is gaining popularity; however, the required size of contrast agents ($\approx 1 \mu\text{m}$), the need for direct tissue contact, and the limited field-of-view (FoV) restrict its utility.

Light, and specifically near-infrared (NIR) light in the biological window (700–900 nm), can be exploited for intraoperative imaging guidance for four important reasons. First, it is invisible, so the look of the surgical field is not altered. Second, it is safe, since the fluence rate (i.e., amount of light) used is small and zoom lenses ensure that the instrument is far from the surgical field. Third, wavelengths in the 800 nm range penetrate relatively deeply into living tissue compared to visible light.¹ Fourth, and most importantly, there has been tremendous recent effort in developing general-purpose NIR fluorophores that can be conjugated to targeting or other molecules, thus creating “contrast agents” matched to any desired surgical application (reviewed in ²).

Our laboratory has previously described NIR fluorescence imaging systems designed for small animal^{3,4} and large animal^{5,6} surgery. The latter is termed the FLARE system, for Fluorescence-Assisted Resection and Exploration. Since our ultimate goal is to translate this technology to the clinic, recent engineering efforts have begun to add hands-free operation and cardiac and respiratory gating,⁷ as well as training tools for surgeons in NIR fluorescence-guided surgery.⁸ In parallel, we have developed robust methods for the conjugation of heptamethine indocyanine NIR fluorophores to small molecules,⁹ peptides,⁹ and proteins.¹⁰ Such conjugates create specialized contrast agents that can be optimized in animal model systems.

Because of immediate clinical need, we have focused on the development of a family of lymphatic tracers optimized for sentinel lymph node (SLN) mapping and resection. Currently, SLN mapping utilizes a combination of radioactive tracer (typically Tc-99m based) and blue dye. Tc-99m-based tracers are used with pre-operative gamma camera imaging and/or an intraoperative handheld gamma probe to generally localize the SLN, and the blue dye to pinpoint the SLN. However, this system adds time to the procedure, requires the involvement of a nuclear medicine physician, exposes patient and caregivers to ionizing radiation, and requires contact (gamma probe) with tissue. The current procedure also has a steep learning curve, requiring up to 60 cases for technical proficiency in breast cancer.¹¹ Until proficiency is attained, up to 16% of SLNs can be missed.¹²

In previous studies, we demonstrated the utility of intraoperative NIR fluorescence imaging for SLN mapping in skin,^{6,10} lung,¹³ pleural space,^{14,15} mammary tissue,⁶ esophagus,¹⁶ stomach,¹⁷ small intestine,^{10,17} and colon.¹⁷ Despite the use of large animals approaching the size of humans, these studies could be criticized for not employing a model system with spontaneous cancer metastatic to regional lymph nodes. We now utilize such a model to complete pre-clinical development of the technology and discuss the factors that will govern its translation to the clinic.

MATERIALS AND METHODS

Intraoperative NIR Fluorescence Imaging System

The principles of the optical path were published in detail previously.⁵ Briefly, a zoom lens with a working distance of 18" directs light to a dichroic mirror, where the visible light (400–700 nm) is deflected to a color video camera (Imitech IMC-80F, IMI Technology Co., Seoul, Korea), and the NIR fluorescence light (>785 nm) is filtered by an emission filter (>795 nm longpass filter) prior to reaching a NIR-sensitive camera (Orca-AG, Hamamatsu, Bridgewater, NJ). The entire optical system is mounted on a shock-resistant aluminum frame, enclosed by a sealed cover measuring 12"W × 12"H × 9"D, and mounted on an adjustable arm that swings out over the surgical field.

NIR excitation light is provided by an array of 10 high-powered (1W) light emitting diodes (LEDs; L-760–66–60, Marubeni Epitex, New York, NY), which are filtered (HHQ750/50x, Chroma Technology, Brattleboro, VT) and focused on the surgical field. White light is provided by an array of four Luxeon III white light diodes (Lumileds, San Jose, CA), from which all NIR wavelengths are filtered out (E680SP, Chroma). The generated fluence rates for NIR excitation and white light range from 0–5 mW/cm² and 0–1 mW/cm², respectively.

Spatial resolution at a field-of-view of 20 × 15 cm is 625 μm, and at a field-of-view of 4 × 3 cm is 125 μm. After computer-controlled (LabVIEW) camera acquisition via custom LabVIEW (National Instruments, Austin, TX) software, anatomic (white light) and functional (NIR fluorescence light) images can be displayed separately and merged. To create a single image that displays both anatomy (color video) and function (NIR fluorescence), the NIR fluorescence image is pseudo-colored in lime green and overlaid with 100% transparency on top of the color video image of the same surgical field. All images are refreshed up to 15 times per second. The entire apparatus is suspended on an articulated arm over the surgical field, thus permitting non-invasive and non-intrusive imaging. Hands-free operation utilizing motorized zoom and focus lenses, a four-pedal footswitch, and a multifunction data acquisition board were described in detail previously.⁷

Organic Lymphatic Tracers

Two different organic tracers that fluoresce at ≈ 800 nm were tested. Indocyanine green (ICG) is a 776 Da di-sulfonated small molecule first FDA approved in 1958 for indicator dilution studies; it is also a NIR fluorophore that has a moderate affinity binding site on human serum albumin (HSA). As we demonstrated previously, ICG adsorbed non-covalently to HSA (ICG:HSA) exhibits a 3.6-fold increase in quantum yield (i.e., brightness), and the 70 kDa complex can be used as a lymphatic tracer.¹⁰ HSA800 is a covalent conjugate of IRDyeTM 800CW NIR dye (CW800; LI-COR, Lincoln, NE; MW 962 Da) to HSA at a molar ratio of 3:1. Its synthesis and purification has been described previously.¹⁰ Final products were resuspended at a final concentration of 10 μM in phosphate-buffered saline, pH 7.4 (PBS) prior to injection.

Inorganic Lymphatic Tracer

Type II NIR fluorescent quantum dots (QDs) were synthesized with a hydrodynamic diameter of 15 nm, a maximal absorption cross-section, an 800 nm fluorescence emission, an aqueous quantum yield ≥9%, and a stable oligomeric phosphine coating as described previously.^{6,18,19} Final products were resuspended at a concentration of 1 μM in PBS prior to injection.

High-Resolution Gel-Filtration Analysis

Gel-filtration analysis with on-line absorbance (200–870 nm) and fluorescence (200–1100 nm) spectrometry was performed as described in detail previously.²⁰ To measure the effect of

serum on hydrodynamic diameter, tracers were diluted in either PBS or 100% calf serum prior to loading of a Superose-6 10/300 GL gel-filtration column (Amersham Biosciences, Piscataway, NJ).

Large Animal Model of Spontaneous Melanoma

Animals were housed in an Association for Assessment and Accreditation of Laboratory Animal Care (AAALAC)-certified facility staffed by full time veterinarians, and were used under supervision of an approved institutional protocol. Sinclair mini-swine of 8–12 weeks of age, and weighing 8–10 kg, were purchased from Sinclair Research Center, Inc. (Columbia, MO). They were housed at a pen temperature of 75–80°F and fed S-9 Sinclair Swine Ration #33133P (Milbank Mills, Chillicothe, MO) and supplements of brown Karo corn syrup. Each animal had 2–4 spontaneous primary melanomas ranging in size from 1–2.5 cm, with most having either microscopic or macroscopic regional nodal metastases. General anesthesia was induced with 10 mg/kg of intramuscular Telazol (Fort Dodge Labs, Fort Dodge, IA). Animals were intubated with a 3 mm endotracheal tube and anesthesia was maintained with 1.5–2% isoflurane/balance O₂ using an MRI-1 ventilator with an expansion valve set (CWE, Inc., Ardmore, PA).

Lymphatic Mapping and SLN Identification

A typical clinical SLN injection protocol was used. 0.4 cc of NIR fluorescent lymphatic tracer resuspended in PBS was taken up into a 1 cc plastic syringe fitted with a 27 gauge, ½" needle. With bevel facing up, each primary melanoma was injected peri-tumorally, in a 4-quadrant pattern, with four 0.1 cc injections. No attempt was made to cannulate lymphatic channels; the needle was simply placed subcutaneously. After injection, the tumor was massaged gently with the thumb four times. Four primary tumors were injected with each lymphatic tracer. Injections, lymphatic tracking, and SLN resection were imaged in real-time, and images archived on the computer. Time from injection to SLN identification was measured using a time-stamp on the archived images. Post-resection inspection of the surgical field was performed using an extended integration time to ensure completeness.

Histological Analysis

Nodal tissue was cryo-sectioned at 6 µm onto Superfrost Plus slides, fixed in 80% acetone/20% water, and stained with hematoxylin and eosin (H&E).

RESULTS

Overview of the Imaging Technology

Although described in detail previously,^{4,5,7} a simplified version of the imaging system is shown in Figure 1A. Two light sources, one for white light and one for NIR fluorescence excitation light illuminate the surgical field. White light reflected from the surgical field is collected by a motorized zoom lens and directed to a color video camera. Normally, there is virtually no NIR fluorescence emission from the surgical field. However, when an exogenous NIR fluorophore is introduced, for example, as a lymphatic tracer, the invisible NIR fluorescent light emitted from the fluorophore is directed to a NIR camera. Both cameras acquire their images simultaneously, permitting “anatomy” (from the color video camera) and “function” (from the NIR camera) to be displayed separately or merged together (discussed below).

Imaging System Hardware Development

Over the last three years, the imaging system hardware has evolved to an easy-to-use and stable optical platform. As shown in Figure 1B, the present FLARE Revision 2 system is contained

within a small footprint (approximately 0.75 ft³), is suspended at a working distance of 18" above the surgical field on an articulated arm, and is sealed within a metal cover that is compatible with sterile drapes. Within the imaging system is a rigid, shock-resistant camera coupler to which is mounted motor control electronics (Figure 1C). A motorized zoom lens provides an adjustable FoV from 15 – 2.3 cm under footswitch control. Technical specifications for the present version of the system are given in Table 1.

Imaging System Software Development

Proper design of the software interface is essential for surgeon satisfaction. Employment of a four-pedal footswitch provides the surgeon with complete control over the FoV, image saving, and image recalling. A software auto-focus algorithm⁷ eliminates the need for manipulation of the focus lens, and cardiac and respiratory gating algorithms eliminate blurring due to motion of the heart, lungs, and viscera. A color video image, otherwise invisible NIR fluorescence image, and pseudo-colored merge of the two, are acquired and displayed simultaneously and in real-time. The overlay of color video and pseudo-colored NIR fluorescence (examples below) is a key feature of the imaging system since it highlights what needs to be resected with high sensitivity and in the context of the surgical anatomy. Unnatural colors for pseudo-colored NIR fluorescence, such as lime green, also provide high visual contrast, especially in the setting of blood.

All images are updated at a maximum of 15 times per second (15 Hz), which is limited only by the data transfer rates of the cameras and the integration time for the NIR fluorescence image. In general, a NIR fluorophore at a concentration of 1 μM, excited with a 5 mW/cm² fluence rate, requires only a 67 msec exposure time for visualization, corresponding to a screen refresh rate of 15 Hz. In our studies, the assistant uses the point-and-click software interface to change camera, screen, and data archiving parameters as requested by the surgeon. Software also includes a cine “loop” mode that displays a time-lapse movie of any procedure recorded by the surgeon.

Large Animal Model System of Spontaneous Melanoma

The Sinclair mini-swine model of spontaneous melanoma was developed in the early 1990s²¹ and has recently been used extensively by Goldberg and colleagues for the optimization of ultrasound-guided SLN mapping.^{22,23} At birth, 54% of animals already have primary melanomas, which increases to 85% at one year.²³ Of importance is that over 70% of primary lesions result in metastases to regional lymph nodes, and spontaneous regression of tumors is uncommon prior to 3 months of age. Coupled with its remarkable histological similarity to human melanoma, this strain of Sinclair mini-swine is an ideal surgical model for the validation of new techniques for SLN mapping. Sinclair swine also represent a “worst case” scenario for optical imaging since they have highly pigmented skin (corresponding to types V–VI human skin) and black fur, which scatters light.

NIR Fluorescent Lymphatic Tracers

Three different lymphatic tracers developed by our laboratory^{6,10} were used in this study. The relative size (i.e., hydrodynamic diameter; HD) of the agents, and their detailed physicochemical and optical properties are presented in Figure 2A. Organic tracers are based upon human serum albumin (HSA), a naturally occurring protein in high abundance in serum. HSA800 is a covalent conjugate of 3 molecules of fluorophore CW800 per molecule of HSA and has a high fluorescent yield. ICG:HSA is a formulation of FDA-approved indocyanine green (ICG) adsorbed non-covalently with HSA. It has a lower total fluorescent yield than HSA800 and NIR QDs, but is composed of two compounds already FDA-approved for other indications. Both of these organic tracers have a HD of ≈ 7 nm, permitting them to quickly enter lymphatics, and travel rapidly to the SLN; they will also flow through the SLN if given

enough time (discussed below). NIR QDs are inorganic/organic hybrid molecules with extreme photostability and high fluorescent yield. They are also engineered to have a large size (≥ 15 nm), which guarantees retention in the SLN.

All tracers have a highly anionic (i.e., negatively charged) surface and a similar charge to mass ratio. As shown in Figure 2B, neither HSA800 nor ICG:HSA are affected by the presence of 100% serum, and maintain their expected HD of 7.4 nm and 7.3 nm, respectively. However, NIR QDs exhibit a previously unexpected size shift in the presence of serum, i.e., as would be expected after subcutaneous injection. Mean HD becomes ≥ 20 nm, with a broadening of the shape distribution, and the appearance of very high molecular weight forms. These gel-filtration results help explain why, in eight separate studies,^{6,10,13,15-17,20,24} NIR QDs are always retained at the first node encountered.

Real-Time NIR Fluorescent SLN Mapping

Each of the 3 lymphatic tracers was injected into $n = 4$ separate primary melanomas in a total of 6 animals. The entire procedure, including injection (Figure 3) could be followed in real-time, with the otherwise invisible NIR fluorescent light identifying all lymphatic channels draining from the primary tumor, and within 15 seconds after injection, identifying the SLN(s). Indeed, the SLN(s) was identified in 100% of injections with all three tracers, although as expected based on total fluorescence yield (Figure 2A), ICG:HSA exhibited slightly lower signal strength than HSA and NIR QDs.

An example SLN mapping procedure using HSA800 is shown in Figure 3. After four peritumoral injections around a large (2 cm) primary tumor on the ventral torso, two separate lymphatic channels were seen, one draining cranially and one caudally. Lymphatic drainage could be followed in real-time, and even pulsations in lymphatic flow could be visualized (Figure 3). Within 15 seconds, one cranial SLN (not shown) and two caudal SLNs (Figure 3) were identified. Importantly, the NIR fluorescent signal from these caudal nodes appeared at the same time, suggesting branching rather than flow through the proximal SLN. Indeed, no flow of tracer was seen beyond the distal SLN. Under image guidance, the two SLNs and a nearby control LN were resected. The surgical field was then inspected using a long integration time (1 second) to ensure that no residual nodal tissue remained.

Pathological Analysis

After tissue resection, the imaging system could be used to dissect non-nodal tissue away from the SLNs and to show the surgical pathologist the sinus entry point (Figure 4A). Tissue from this area was then analyzed histologically. As shown in Figure 4B, both the proximal and distal SLNs were found to harbor metastatic tumor cells, while the nearby control LN had none present.

DISCUSSION

Optical imaging, and especially NIR fluorescence imaging, has several advantages for oncologic surgery. Autofluorescence of tissue and blood is relatively low in the 800 nm wavelength range.^{2,8} By adding an exogenous fluorophore, a bright spot on a black background is thus created, permitting high sensitivity detection of any desired target within the surgical field. The imaging system described in this study is a stable optical platform that utilizes safe NIR diode excitation, provides simultaneous overlay of color anatomy and NIR fluorescence, is positioned safely above the patient without requiring any contact, and has no moving parts.

Since even NIR light is scattered in living tissue, the depth of light penetration might be expected to be a major obstacle to optical imaging in surgery; however, this doesn't seem to

be a major issue. First, the surgeon can follow the lymphatic channels from the injection site towards the SLN, so the direction is always known. Second, because tissue background is so low, tracers can be detected below relatively thick (≈ 0.5 –1 cm) tissue⁶ and below up to 5 cm of lung.¹³ Of course, on the surface of the tissue, the appearance of the SLN will be “blurred” by scatter and appear larger than it really is (see, for example, Figure 3), but its exact location, and therefore the exact location of the surgical incision, will still be known. Finally, it will likely be possible to adapt newer optical techniques, such as frequency-domain photon migration (reviewed in ^{25,26}), to our imaging system to improve detectability into the 2–4 cm range.

This study essentially completes pre-clinical development of NIR fluorescent SLN mapping and resection. Using large animal model systems, we have now demonstrated optimized protocols for SLN mapping of spontaneous melanoma, skin,^{6,10} lung,¹³ pleural space,^{14,15} mammary tissue,⁶ esophagus,¹⁶ stomach,¹⁷ small intestine,^{10,17} and colon.¹⁷ Using this technology, the need for radioactivity and blue dye is eliminated, and the SLN is typically identified within seconds.

Our studies also found important differences among lymphatic tracers; these differences have implications for the translation of this technology to the clinic. Organic tracers, like those from this study based on albumin, are advantageous because of their availability and biocompatibility. Inorganic/organic hybrid NIR QDs are brighter and remarkably stable to photobleaching, but have yet to undergo proper toxicological screening. From this study, it also appears that type II NIR QDs with a purely anionic coating bind serum proteins and shift their size to 20 nm and greater, whereas zwitterionic molecules with the same concentration of anions, do not. This is an important finding because the small agents, such as HSA800 and ICG:HSA, often identify lymphatic branches (see 16 for detailed description and Figure 3 of this study) and small SLNs, whereas we have never seen branching with NIR QDs and other large HD tracers. The importance of this point cannot be overstated. As shown in Figures 3 and 4, the other (distal) SLN was extremely small (only 2 mm) yet harbored metastatic cells. For eventual use in humans, the goal must be to find all SLNs, regardless of their size and the size of the connecting lymphatic channels. Since flow in lymphatic channels is pulsatile with heartbeat and respiration, and channels are often collapsed, the smaller HD particles might have an advantage. Moreover, since the SLN is identified within seconds using NIR fluorescence imaging, the probability of tracer flow through the SLN to the next tier is minimized. At least in the case of the Sinclair melanoma model, SLNs from all 12 primary tumors studied harbored either micro- or macrometastases, suggesting an extremely low false-negative rate for all three lymphatic tracers.

The clinical translation of this technology for SLN mapping is imminent. At the present time, the ICG:HSA formulation offers the significant advantage that both components are already FDA-approved for other indications, the amount of each component needed for SLN mapping is orders of magnitude lower than the doses of each used for these other indications, and total fluorescence yield in a serum environment is reasonably high. Within the organic class of SLN tracers, HSA800 would provide an additional 2.2-fold improvement in fluorescent yield, but HSA800, like ICG:HSA, would have a hydrodynamic diameter that permits passage through the SLN if too much time elapses after injection.^{10,14} Quantum dots, although still years away from clinical translation, provide the highest fluorescence yield, as well as a definable hydrodynamic diameter that ensures complete retention in the first lymph encountered.^{6,10,13,15-17,20}

Newer NIR fluorescent contrast agents, such as HSA800,¹⁰ are being developed at a relatively high rate, and the future promises NIR fluorescent contrast agent targeted to a variety of cancers.²⁷ Indeed, tumor-specific targeting should permit real-time assessment of tumor

margins and identification of occult metastases within the surgical field. The technology can also help the surgeon to avoid nerves, blood vessels, etc. during cancer resection. The availability of tissue- and disease-targeted NIR fluorophores will likely have a lag of 3–5 years due to a variety of regulatory factors (reviewed in²⁸). Nevertheless, ICG:HSA, and ICG alone,^{5,29,30} will undoubtedly have many clinical applications and will hopefully fill the void.

It should be emphasized that the NIR fluorescence imaging system described in this study might eventually play a dual role in patient management. It not only provides the surgeon with real-time image guidance during any oncologic procedure, but also assists the surgical pathologist. First, the specimen can be trimmed under image guidance. Second, the particular area of interest, e.g., sinus entry point of the SLN, can be found and sectioned at high-resolution to find micrometastases. Finally, since NIR fluorophores withstand frozen sectioning,^{6,16} a NIR fluorescence microscope³¹ can be used to correlate the resected target with at least three other fluorescence channels of biologic markers.

ACKNOWLEDGMENTS

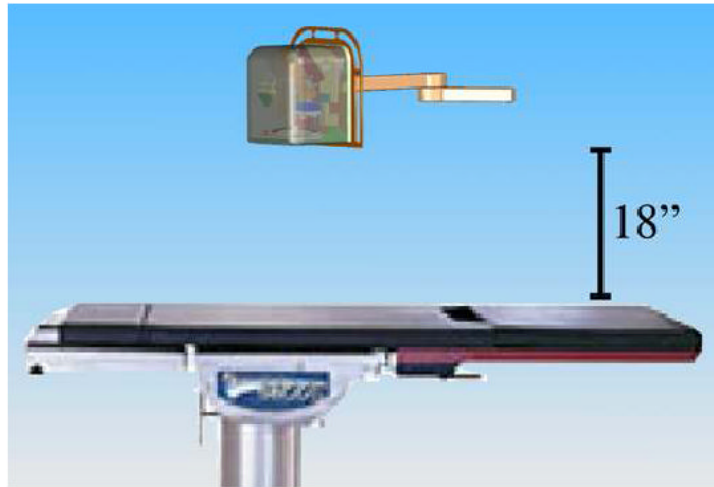
We thank Rita G. Laurence for assistance with animal anesthesia, Alec M. De Grand for maintenance of imaging system software, Daniel A. Brown for cryo-sectioning, Barbara L. Clough for editing, and Grisel Rivera for administrative assistance. This work was supported in part by the National Science Foundation-Materials Research Science and Engineering Center Program under grant DMR-0213282 (MGB), NIH grants #R01-CA-115296 (JVF), R21-CA-110185 (JVF), and R33-EB-000673 (JVF and MGB), and an Application Development Award (JVF) from the Center for Integration of Medicine and Innovative Technology (CIMIT).

REFERENCES

1. Lim YT, Kim S, Nakayama A, Stott NE, Bawendi MG, Frangioni JV. Selection of quantum dot wavelengths for biomedical assays and imaging. *Mol Imaging* 2003;2:50–64. [PubMed: 12926237]
2. Frangioni JV. In vivo near-infrared fluorescence imaging. *Curr Opin Chem Biol* 2003;7:626–34. [PubMed: 14580568]
3. Zaheer A, Lenkinski RE, Mahmood A, Jones AG, Cantley LC, Frangioni JV. In vivo near-infrared fluorescence imaging of osteoblastic activity. *Nat Biotechnol* 2001;19:1148–54. [PubMed: 11731784]
4. Nakayama A, del Monte F, Hajjar RJ, Frangioni JV. Functional near-infrared fluorescence imaging for cardiac surgery and targeted gene therapy. *Mol Imaging* 2002;1:365–77. [PubMed: 12940233]
5. De Grand AM, Frangioni JV. An operational near-infrared fluorescence imaging system prototype for large animal surgery. *Technol Cancer Res Treat* 2003;2:553–62. [PubMed: 14640766]
6. Kim S, Lim YT, Soltesz EG, et al. Near-infrared fluorescent type II quantum dots for sentinel lymph node mapping. *Nat Biotechnol* 2004;22:93–7. [PubMed: 14661026]
7. Gioux S, De Grand AM, Lee DS, Yazdanfar S, Idoine JD, Lomnes SJ, Frangioni JV. Improved optical sub-systems for intraoperative near-infrared fluorescence imaging. *Proc. of SPIE* 2005;6009:39–48.
8. De Grand AM, Lomnes SJ, Lee DS, et al. Tissue-like phantoms for near-infrared fluorescence imaging system assessment and the training of surgeons. *J Biomed Opt* 2006;11:14007.
9. Zaheer A, Wheat TE, Frangioni JV. IRDye78 conjugates for near-infrared fluorescence imaging. *Mol Imaging* 2002;1:354–64. [PubMed: 12926231]
10. Ohnishi S, Lomnes SJ, Laurence RG, Gogbashian A, Mariani G, Frangioni JV. Organic alternatives to quantum dots for intraoperative near-infrared fluorescent sentinel lymph node mapping. *Mol Imaging* 2005;4:172–81. [PubMed: 16194449]
11. Mariani G, Moresco L, Viale G, et al. Radioguided sentinel lymph node biopsy in breast cancer surgery. *J Nucl Med* 2001;42:1198–1215. [PubMed: 11483681]
12. Schirrmester H, Kotzerke J, Vogl F, et al. Prospective evaluation of factors influencing success rates of sentinel node biopsy in 814 breast cancer patients. *Cancer Biother Radiopharm* 2004;19:784–90. [PubMed: 15665628]
13. Soltesz EG, Kim S, Laurence RG, et al. Intraoperative sentinel lymph node mapping of the lung using near-infrared fluorescent quantum dots. *Ann Thorac Surg* 2005;79:269–77. [PubMed: 15620956] discussion 269–77

14. Parungo CP, Ohnishi S, De Grand AM, et al. In vivo optical imaging of pleural space drainage to lymph nodes of prognostic significance. *Ann Surg Oncol* 2004;11:1085–92. [PubMed: 15545502]
15. Parungo CP, Colson YL, Kim SW, Kim S, Cohn LH, Bawendi MG, Frangioni JV. Sentinel lymph node mapping of the pleural space. *Chest* 2005;127:1799–804. [PubMed: 15888861]
16. Parungo CP, Ohnishi S, Kim SW, et al. Intraoperative identification of esophageal sentinel lymph nodes with near-infrared fluorescence imaging. *J Thorac Cardiovasc Surg* 2005;129:844–50. [PubMed: 15821653]
17. Soltesz EG, Kim S, Kim SW, et al. Sentinel lymph node mapping of the gastrointestinal tract by using invisible light. *Ann Surg Oncol* 2006;13:386–96. [PubMed: 16485157]
18. Kim SW, Kim S, Tracy JB, Jasanoff A, Bawendi MG. Phosphine oxide polymer for water-soluble nanoparticles. *J Am Chem Soc* 2005;127:4556–7. [PubMed: 15796504]
19. Kim S, Fisher B, Eisler HJ, Bawendi M. Type-II quantum dots: CdTe/CdSe(core/shell) and CdSe/ZnTe(core/shell) heterostructures. *J Am Chem Soc* 2003;125:11466–7. [PubMed: 13129327]
20. Frangioni JV, Kim SW, Ohnishi S, Kim S, Bawendi MG. Sentinel lymph node mapping with type II quantum dots. *Methods Mol Biol*. 2006In Press
21. Misfeldt ML, Grimm DR. Sinclair miniature swine: an animal model of human melanoma. *Vet Immunol Immunopathol* 1994;43:167–75. [PubMed: 7856049]
22. Goldberg BB, Merton DA, Liu JB, Murphy G, Forsberg F. Contrast-enhanced sonographic imaging of lymphatic channels and sentinel lymph nodes. *J Ultrasound Med* 2005;24:953–65. [PubMed: 15972710]
23. Goldberg BB, Merton DA, Liu JB, et al. Sentinel lymph nodes in a swine model with melanoma: contrast-enhanced lymphatic US. *Radiology* 2004;230:727–34. [PubMed: 14990839]
24. Kim SW, Zimmer JP, Ohnishi S, Tracy JB, Frangioni JV, Bawendi MG. Engineering InAs(x)P(1-x)/InP/ZnSe III-V alloyed core/shell quantum dots for the near-infrared. *J Am Chem Soc* 2005;127:10526–32. [PubMed: 16045339]
25. Ntziachristos V, Bremer C, Weissleder R. Fluorescence imaging with near-infrared light: new technological advances that enable in vivo molecular imaging. *Eur Radiol* 2003;13:195–208. [PubMed: 12541130]
26. Sevick-Muraca EM, Houston JP, Gurfinkel M. Fluorescence-enhanced, near infrared diagnostic imaging with contrast agents. *Curr Opin Chem Biol* 2002;6:642–50. [PubMed: 12413549]
27. Humblet V, Lapidus R, Williams LR, et al. High-affinity near-infrared fluorescent small-molecule contrast agents for in vivo imaging of prostate-specific membrane antigen. *Mol Imaging* 2005;4:448–62. [PubMed: 16285907]
28. Frangioni JV. Translation of *in vivo* diagnostics from bench to bedside in the era of personalized medicine. *Nat Biotechnol*. 2006In Press
29. Balacumaraswami L, Abu-Omar Y, Choudhary B, Pigott D, Taggart DP. A comparison of transit-time flowmetry and intraoperative fluorescence imaging for assessing coronary artery bypass graft patency. *J Thorac Cardiovasc Surg* 2005;130:315–20. [PubMed: 16077393]
30. Sekijima M, Tojimbara T, Sato S, et al. An intraoperative fluorescent imaging system in organ transplantation. *Transplant Proc* 2004;36:2188–90. [PubMed: 15518796]
31. Nakayama A, Bianco AC, Zhang CY, Lowell BB, Frangioni JV. Quantitation of brown adipose tissue perfusion in transgenic mice using near-infrared fluorescence imaging. *Mol Imaging* 2003;2:37–49. [PubMed: 12926236]
32. Sugio S, Kashima A, Mochizuki S, Noda M, Kobayashi K. Crystal structure of human serum albumin at 2.5 Å resolution. *Protein Eng* 1999;12:439–46. [PubMed: 10388840]
33. Petitpas I, Bhattacharya AA, Twine S, East M, Curry S. Crystal structure analysis of warfarin binding to human serum albumin: anatomy of drug site I. *J Biol Chem* 2001;276:22804–9. [PubMed: 11285262]

A.



B.

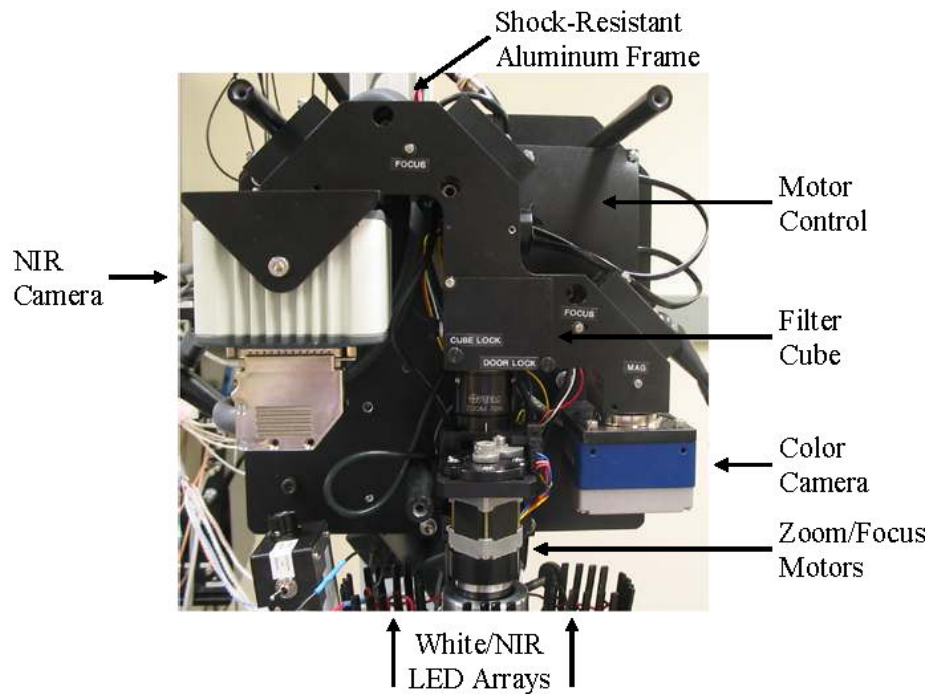


Figure 1. FLARE Revision 2 Intraoperative NIR Fluorescence Imaging System

A. White light and invisible NIR fluorescence excitation light illuminate the surgical field. Reflected white light (i.e., surgical anatomy) is directed to a color video camera, while invisible NIR fluorescent light (from the introduced NIR fluorophore) is directed simultaneously to a NIR camera. The independent light paths for white light (solid arrows) and invisible NIR light (dotted arrows) are shown.

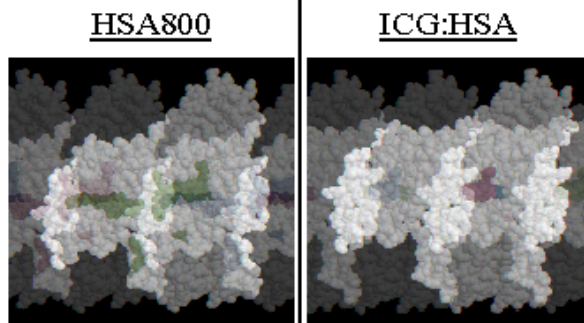
B. The FLARE imaging system is completely self-contained and is mounted on an articulated arm that swings over the surgical field. Working distance of the optics is 18" from the subject. The schematic is drawn to scale relative to a Skytron Model 6001 operating room table.

C. Beneath the aluminum cover are the sub-systems for which specifications are provided in Table 1. All parts mount to a rigid, shock-resistant aluminum frame, which ensures alignment of the two cameras.

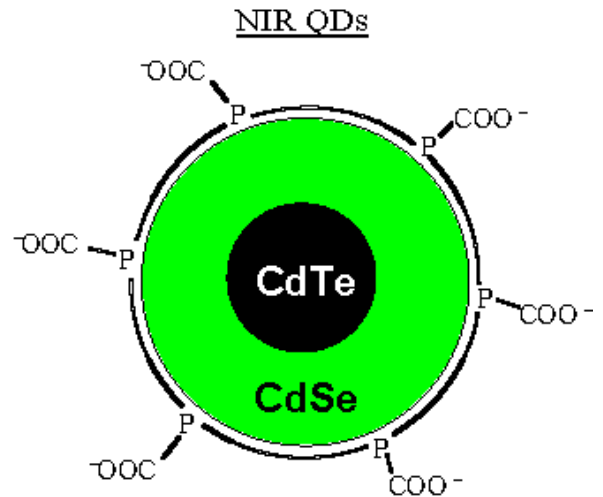
A.

Summary of NIR Fluorescent Lymphatic Tracers (Drawn to Scale)

Organic



Inorganic/Organic Hybrid



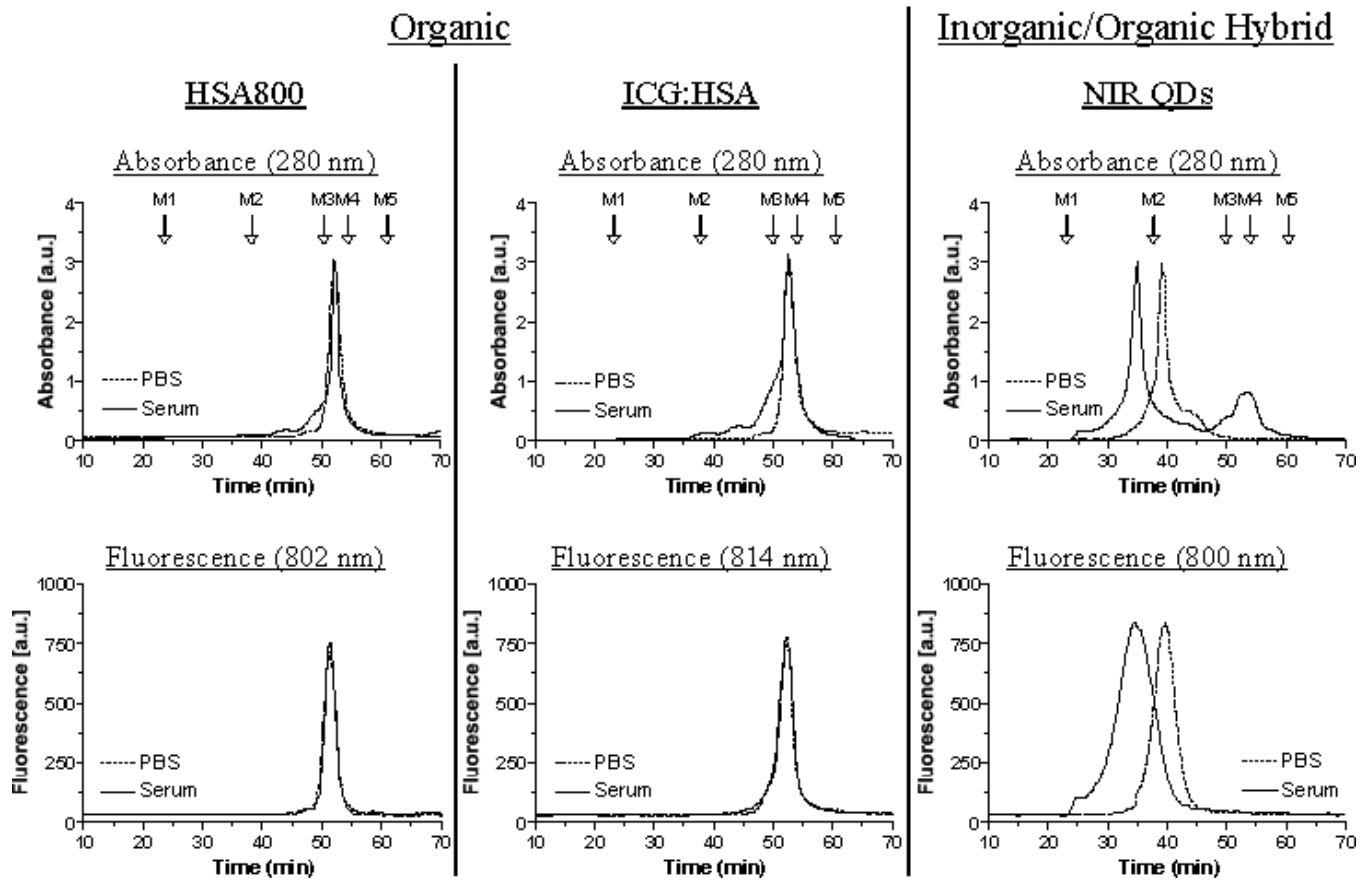
Molecular Weight: 70 kDa
 Diameter (PBS): 7.4 nm
 Diameter (Serum): 7.4 nm
 Charge to Mass Ratio ($\times 10^{-3}$): -3.9
 Excitation Max. (Serum): 784 nm
 Emission Max. (Serum): 802 nm
 Quantum Yield (Serum): 12%
 Relative Total Yield (Serum): 2.2
 Photobleach: Yes

67 kDa
 7.3 nm
 7.3 nm
 -3.0
 800 nm
 814 nm
 9%
 1.0
 Yes

440 kDa (gel-filtration equivalent)
 15 nm
 20 nm
 ≈ -1.0
 n/a (broadband)
 800-860 nm (tunable)
 9%
 2.9
 No

B.

Effective Hydrodynamic Diameter in Serum



Original Quantum Dot Figure

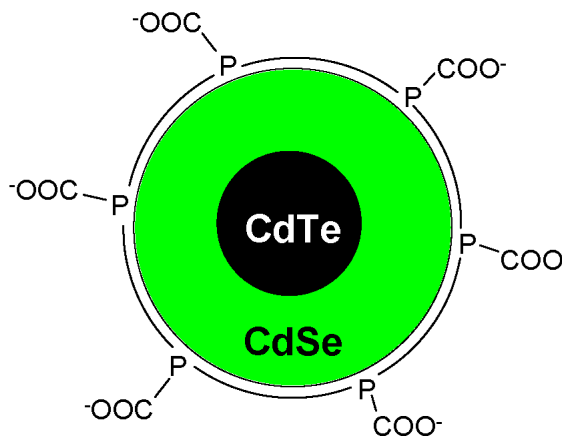
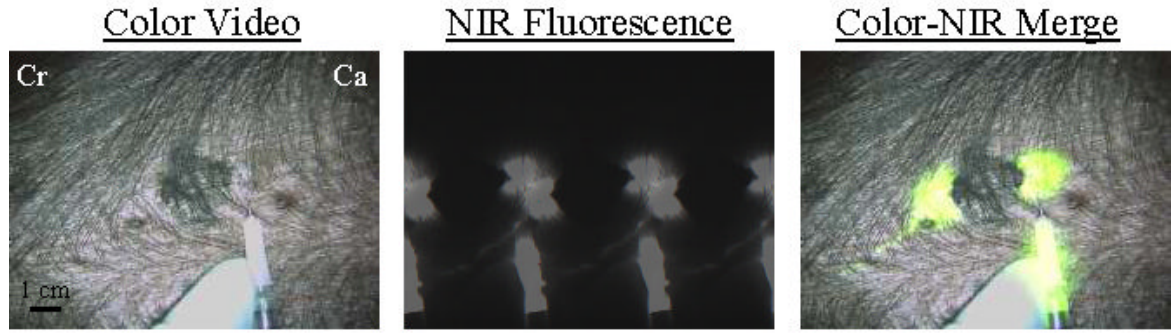


Figure 2. Physicochemical and Optical Properties of NIR Fluorescent Tracers for Image-Guided SLN Mapping and Resection

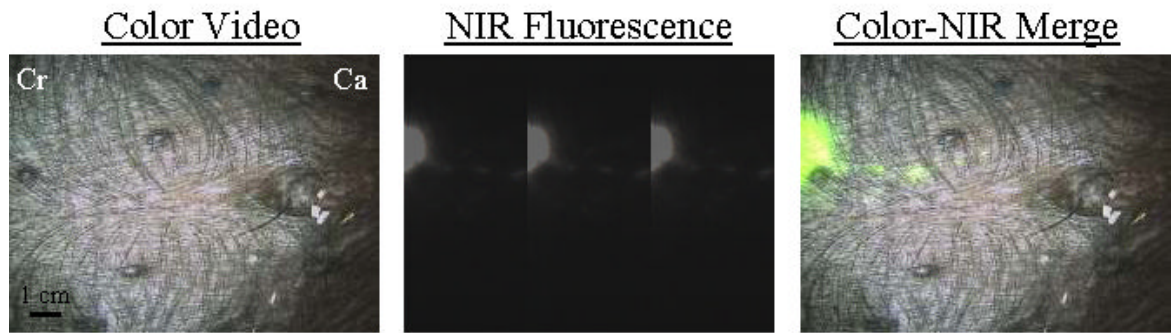
A. Organic lymphatic tracers include HSA800 (left) and ICG adsorbed non-covalently to HSA (ICG:HSA; middle). The crystal structure of HSA³² is shown in white, and the position of NIR fluorophores in green. The three CW800 conjugation sites of HSA800 are adapted from Ohnishi et al.¹⁰ and correspond to Lys162, Lys274, and Lys557. The ICG binding site is presumed to be HSA site I³³ based on the similarity of its chemical structure to other site I ligands. NIR QDs are an inorganic/organic hybrid having a semiconductor metal core and a highly anionic organic coating derived from oligomeric phosphines. All three tracers are drawn to scale, based on their hydrodynamic diameters measured using gel-filtration chromatography. Below each tracer are its physicochemical and optical properties.

B. The effect of serum proteins on hydrodynamic diameter was measured using high-resolution gel-filtration with on-line absorbance and fluorescence spectrometry. Lymphatic tracers were analyzed after dilution in PBS (dashed curves) or 100% serum (solid curves). Absorbance at 280 nm (top) is used to show the position of all proteins present. Molecular weight markers M1 (blue dextran; 2 MDa, 43.4 nm HD), M2 (thyroglobulin; 669 kDa, 18.8 nm HD), M3 (γ -globulin; 158 kDa, 11.1 nm HD), M4 (ovalbumin; 44 kDa, 6.1 nm HD), and M5 (myoglobin; 17 kDa, 3.8 nm HD) are shown by arrows. Fluorescence at the peak emission wavelength (bottom) is shown for each tracer.

Injection (T = 0)



Lymphatic Channels (T = 5 secs)



Identification of SLNs (T = 15 secs)

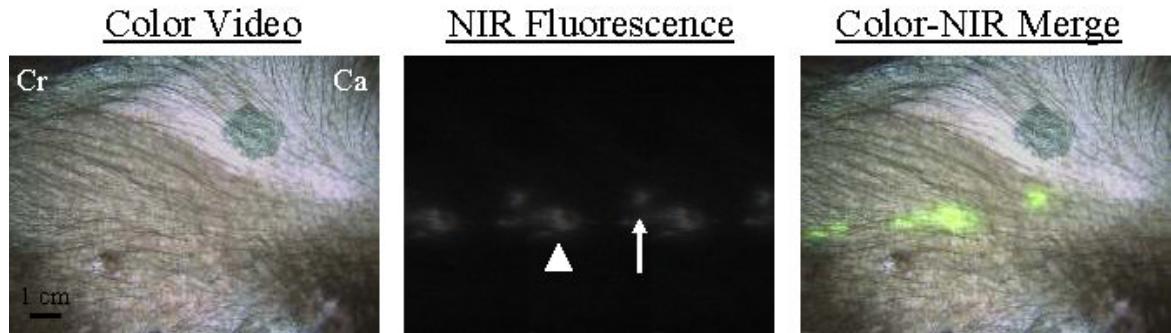
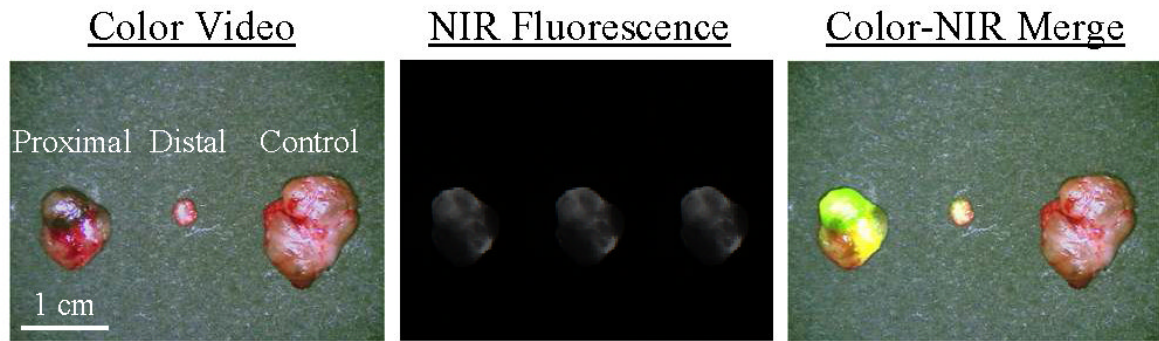


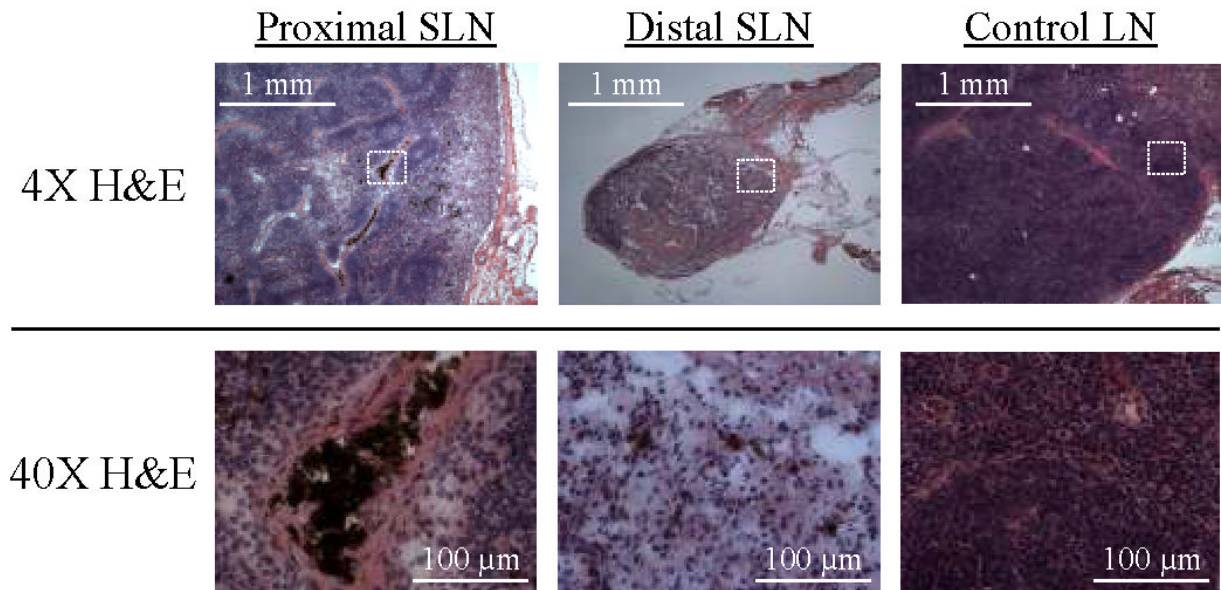
Figure 3. Real-Time Intraoperative NIR Fluorescent Sentinel Lymph Node Mapping

At T = 0, four peri-tumoral, subcutaneous injections of 1 nmol of HSA800 were made around a primary melanoma on the ventral left torso. Two dominant lymphatic channels, one cranial (Cr) and one caudal (Ca) were found. The caudal channel was followed (T = 5 secs) until two SLNs were identified at T = 15 secs. Images shown include color video (left), NIR fluorescence (middle) and a pseudo-colored (lime green) merge of the two (right). Exposure time (67 msec) and normalizations were the same for all NIR fluorescence images.

A.

Surgical Pathology (T = 1 min)

B.

Histology**Figure 4. Image-Guided Pathological Analysis of Resected SLNs**

A. Surgical Pathology. After image-guided resection of the two SLNs and a control LN from the animal in Figure 3, specimens could be re-imaged and trimmed by a surgical pathologist under image guidance. The sinus entry point could also be identified and the LN processed for maximal likelihood of finding metastases.

B. Histology. H&E staining of each LN from Figure 4A revealed metastases in both the proximal and distal SLNs, as evidenced by the melanin-containing brown cells with large nuclei, but not the control LN. The dotted white box in each 4X image corresponds to the field shown in the 40X image.

Table 1

FLARE Revision 2 Imaging System Specifications

<u>Physical</u>	
Footprint:	12" W × 12" H × 9" D (0.75 ft ³)
Weight:	25 lbs.
Mechanical:	Articulated Arm
<u>Optics and Cameras</u>	
Working Distance:	15" – 18"
Surgical Field of View:	15 W × 11.25 H cm to 2.3 W × 1.7 H cm (adjustable)
System Resolution:	625 μm (x,y) to 125 μm (x,y) based on based on FoV
Color Video Camera:	Imitech IMC-80F (Non-cooled, 1/3" format, 15 fps, IEEE-1394)
NIR Camera:	Orca-AG (Cooled -30°, 2/3" format, 15 fps, IEEE-1394)
NIR Image Integration:	10 ms — 2 sec (adjustable)
<u>Lighting</u>	
White Light:	Luxeon III LEDs × 4 (700 mA max) w/ ≤ 680 nm filtration
NIR Excitation Light:	Epitex L760-66-60 LEDs × 10 (700 mA max) w/ 725-775 nm filtration and focusing
<u>Software and Control</u>	
Synchronization:	Cardiac and respiratory gating
Hands-Free Operation:	Auto-focus, footswitch
Surgeon Controls:	4-pedal footswitch (Zoom In, Zoom Out, Save, Recall)
Assistant Controls:	All system functions via keyboard and mouse
